Nanofluidic Ionic Diodes. Comparison of Analytical and Numerical Solutions

Ivan Vlassiouk,[†,*] Sergei Smirnov,[‡] and Zuzanna Siwy[†]

[†]Department of Physics and Astronomy, University of California, Irvine, California 92697, and [‡]Department of Chemistry and Biochemistry, New Mexico State University, Las Cruces, New Mexico 88003

ABSTRACT Recently reported experimental and theoretical studies of nanofluidic nonlinear devices, such as bipolar and unipolar ionic diodes, have yet to answer the question about the possibility of their further miniaturization. In this Article, we theoretically investigate the effects of size reduction, applied bias, and solution ionic strength in such devices. We compare the numerical solutions of the Poisson, Nernst—Planck (PNP), and Navier—Stokes (NS) equations with their one-dimensional, analytical approximations. We demonstrate that the contribution of electroosmosis is insignificant and find analytical approximations to PNP for bipolar and unipolar diodes that are in good agreement with numerical 3D solutions. We identify the minimal dimensions for such diodes that demonstrate ion current rectification behavior and demonstrate the importance of the edge effect in very short diodes.

KEYWORDS: nanochannel · nanofluidic diode · nanofluidic electronics · bipolar and unipolar devices · Poisson—Nernst—Planck equations

Controlling ion flow through nanochannels has a broad range of possible applications in various fields. One of the most attractive ways to realize such control is *via* electrostatic interactions. If at least one dimension of a nanofluidic channel (height or width) is comparable to the Debye length, then the surface electric potential can greatly influence the concentrations and type of ions in the nanochannel. It is the surface potential that provides an opportunity to influence the ionic flux through the channel. There are two ways to alter the surface potential. In the first approach, the intrinsic surface charge is defined by the properties of the surface groups. This is "passive" control of the electric potential since it is only affected by the pH and ionic concentration of the bulk solution and can be altered by changing the density/chemical composition of the groups on the channel's walls. When a nanochannel is covered by a conductive layer, an "active" way of surface potential control can be achieved. This conductive layer can be electrically addressed; therefore, a potential difference between the electrolyte solution and the nanochannel walls can be applied, rendering the surface positively or negatively charged.

Both these approaches of altering the surface potential in a nanochannel have been applied for constructing nanofluidic analogues of semiconductor devices. Ionic filters that allow selective transport of either cations or anions were one of the first reported ion controlling systems.[1,2]

More complex ionic devices can be achieved by introducing an uneven distribution of the surface potential in the channel. An immediate consequence of this broken symmetry is the formation of an ionic rectifier. This asymmetry can be achieved through either nanochannel shape or charge, or a combination of both. Asymmetrical nanopore geometry, for example, with conically shaped pores,[3] shows ionic current rectification. Asymmetrical surface charge distributions[4–6] can form a junction similar to the p—n semiconductor junction (*i.e.*, a nanofluidic diode). This kind of junction was originally realized in bipolar membranes,[7–10] but recently received renewed interest through its realization in single nanochannels. These nanofluidic diodes, similar to their semiconductor counterparts, allow the flow of ionic current in one direction, blocking the flow of ions in the other.[4,5,11,12] Controlling the current and the ion flux in both directions can also be realized in nanofluidic transistors such as bipolar[11–13] or field-effect nanofluidic transistors.[14–16]

The majority of nanofluidic nonlinear devices have been realized using long nanochannels with large aspect ratios. Recent improvements in nanofabrication techniques offer manufacturing precision down to 1 nm and could allow the construction of low aspect ratio single

*Address correspondence to ivlassio@uci.edu.

Received for review May 19, 2008 and accepted July 02, 2008.

Published online July 22, 2008.
10.1021/nn800306u CCC: $40.75

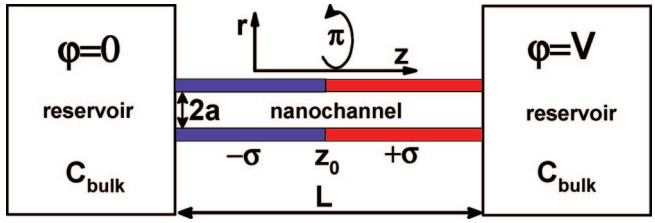

Figure 1. Schematic of a nanofluidic diode. A nanochannel of radius *a* and length *L* is connected to two reservoirs characterized by the bulk concentration of KCl − C_{bulk}. The left reservoir is grounded, whereas the right reservoir is under potential $-V$. Bipolar diode (BP): from $z = 0$ to z_0 $\sigma(z) = -\sigma$, while from $z = z_0$ to $z = L$ $-\sigma(z) = \sigma$. Unipolar diode (UP): from $z = 0$ to z_0 $\sigma(z) = -\sigma$, while from $z = z_0$ to $z = L$ $-\sigma(z) = 0$. For $\sigma > 0$, the potential $V < 0$ corresponds to the open (forward) state of the diodes and $V > 0$ to the closed (reverse) state. For the majority of considerations $z_0 = L/2$.

nanochannels and their arrays.[17–20] Longitudinal shrinkage is an attractive approach to further miniaturize such nanofluidic analogues of semiconductor devices, and we wish to explore the physical limitations of such size reduction. The Leburton group at the University of Illinois at Urbana—Champaign theoretically analyzed the double-conical geometry for short nanochannels,[21–23] which has been experimentally realized by electron beam drilling in silicon-based materials.[20–25] Chen *et al.*[25] experimentally observed ion current rectification in nanopores with a diameter of ~15 nm and a length of ~40 nm that were prepared by ion milling. The rectification was pH-dependent and quite large, but it disappeared after uniform surface modification by Al_2O_3, performed using the atomic layer deposition technique. The Al_2O_3 treatment eliminated the uneven charge (and perhaps shape as well) distribution brought about by the ion milling fabrication process. There have been no reports so far that experimentally verified rectification behavior of nanopores of just a few nanometers in length. Here we present our analysis of unipolar and bipolar diodes built on the basis of cylindrical nanopores.

Most recent experimental data are available for synthetic nanopore ionic diodes with large aspect ratios over 10[3],[4,5] but diodes based on protein channels that have much smaller aspect ratios of ~5 have been constructed as well.[26,27] The artificial devices appear to have superior rectification properties, at least as judged by the ratio of currents recorded for opposite voltages of the same magnitude. It is important for the further development of ionic devices to clarify whether this difference is defined solely by the length of the pore.

The majority of publications dealing with nanofluidic diodes rely only on numerical calculations, whereas much less attention is paid to utilizing analytical models. Following our previous analysis of conductance through uniformly charged nanopores,[34] here we compare full numerical solutions with analytical approximations for nanofluidic ionic diodes. We present derivation of 1D analytical approximations for two types of ionic diodes built on single nanochannels with nonuniformly charged walls: (i) bipolar diodes consisting of a junction between positively and negatively charged parts, and (ii) unipolar diodes containing a charged zone in contact with a neutral part. Theoretical treatments of the nanofluidic diodes as well as the equations derived in this Article have a striking similarity to the corresponding solid-state devices. We show similarities of an ionic bipolar diode to a p–n semiconductor junction and similarities of a unipolar ionic diode to a Schottky solid-state diode.

Description of Ion Current through Nanofluidic Diodes. Each nanofluidic device under consideration is based on a single nanochannel with length *L* and radius *a*, as shown in Figure 1. The nanochannel has a surface charge varying along the channel's *z*-axis, $\sigma(z)$, for which we neglect the possibility of depending on electrolyte and nanochannel radius (*i.e.*, no surface charge regulation).[28,29] The nanochannel is connected to reservoirs with identical bulk concentrations of KCl − C_{bulk}.

The Poisson−Nernst−Planck (PNP) equations coupled with the Navier−Stokes (NS) equation describe such systems and are written as

$$\begin{cases} \varepsilon_0 \varepsilon \Delta\varphi = e(C_+ - C_-) \\ J_i = -D_i\left(\nabla C_i + \dfrac{z_i e C_i}{k_B T}\nabla\varphi\right) \\ \nabla\cdot(C_i u + J_i) = 0 \\ \nabla\cdot u = 0 \\ u\nabla u = \dfrac{1}{\rho}[-\nabla p + \nu\nabla^2 u - (C_+ - C_-)\nabla\varphi] = 0 \end{cases} \quad (1)$$

In the Poisson equation, ϵ_0 is the permittivity of vacuum, dielectric constant $\epsilon = 80$, *e* is the electron charge, C_+ and C_- are the ionic number densities (concentrations) of positive (K^+) and negative (Cl^-) ions, respectively, and φ is the electrical potential. The Nernst−Planck (NP) equation describes the flux J_i, of an ion *i* with charge z_i, due to a concentration gradient and the drift in the potential gradient, both of which are proportional to the ions' diffusion coefficient. The diffusion coefficients, D_i, are presumed to be identical and equal, 2×10^{-9} m^2/s for both ions. The mobilities of the ions are then calculated as $\mu_i = eD_i/k_BT$, where k_B is the Boltzmann constant. The continuity condition (the third equation) links the solution velocity vector, *u*, with the ionic flux. The solution is presumed to be incompressible (the fourth equation). The Navier−Stokes (NS) equation completes the set but is often omitted with the assumption of no movement for the solution, $u = 0$, when no external pressure, *p*, is applied. Since appearance of nonzero *u* under electric field and with no pressure applied is called electroosmosis, exclusion of NS is usually referred to as an omission of electroosmosis.

Boundary conditions finalize the problem description. The electrical potential on the farthest borders in the left and right reservoirs were set to 0 and V, respectively, as shown in Figure 1. The boundary condition: $d\varphi/dr|_{r=a} = \sigma/\varepsilon\varepsilon_0$ was applied at the walls. For the Navier−Stokes equation, the solution velocity at the walls was set to zero, $u(a) = 0$, and the density and viscosity of pure water, $\rho = 1000$ kg/m^3 and $\nu = 1$ mPa · s, were used.

As we will show below, the contribution of electroosmosis is small compared to the diffusive components. Neglecting NS ($u = 0$) significantly simplifies the equation set (eq 1) to what is abbreviated as the PNP approximation:

$$\begin{cases} \varepsilon_0\varepsilon\Delta\varphi = e(C_+ - C_-) \\ \nabla\cdot\left(\nabla C_i + \dfrac{z_i e C_i}{k_B T}\nabla\varphi\right) = 0 \end{cases} \quad (2)$$

with zero bias applied, PNP (eq 2) reduces further to the Poisson−Boltzmann (PB) equation:

$$\Delta\varphi' = k^2 \sinh\varphi' \quad (3)$$

where $\varphi' = e\varphi/k_BT$ is the dimensionless electric potential and $k = [2e^2C_{bulk}/\varepsilon_0\varepsilon k_BT]^{1/2}$ is the inverse Debye length. Both the PNP and PB equations are mean-field approximations, and their application in very narrow channels is difficult to justify. However, for the nanochannel dimensions used in this study ($a > 1$ nm), it was demonstrated that the mean-field PNP approach shows the same results as obtained by Brownian dynamics simulations.[30,31]

Both the PNP and PB equations can be routinely solved numerically for an arbitrary shape of a nanochannel and charge distribution. However, the exact analytical solution of the PB equation is not even known for the cylindrical geometry. If the electric potential is small, eq 3 may be linearized to $\Delta\varphi' = k^2\varphi'$, which is known as the Debye−Huckel (DH) approximation. Knowing the electric potential distribution at zero bias, the corresponding ionic concentrations are calculated as $C_\pm = C_{bulk}\exp[\pm\varphi']$. The analytical solution of the DH equation for a cylinder has been known for years,[32] but it greatly overestimates the potential for small values of ka, introducing a substantial error. Recently, Petsev and Lopez (PL) derived an approximate solution[33] for the PB equation in a cylindrical nanochannel, which agrees better with the numerical solutions, especially for $ka \geq 4$.

Because of PNPs' complexity in a three-dimensional (3D) formulation, we will seek 1D analytical approximations. In the 1D description of the problem, there is always a concentration difference between the majority carriers ($C_>(z)$ − counterions) − the ions of the opposite charge to that of the walls, and the minority carriers ($C_<(z)$ − co-ions). These concentrations are averaged over the channel cross section and thus are functions of z only. Because of the electroneutrality condition, the concentration difference can be calculated as $\Delta C(z) = C_>(z) - C_<(z) = 2|\sigma(z)|/ea$. The concentrations at zero bias can then be written as

$$\begin{cases} C_>' = 0.5(\Delta C' + C_D') \\ C_<' = 0.5(-\Delta C' + C_D') \\ C_D' = \sqrt{\Delta C'^2 + 4} \end{cases} \quad (4)$$

where the prime refers to dimensionless concentrations, that is, normalized by C_{bulk}. The Donnan concentration, C_D, represents the total ionic concentration inside the nanochannel, $C_D = C_> + C_<$.

An abrupt change in the surface charge results in a similarly abrupt change in the electric potential:

$$\varphi_{right} - \varphi_{left} = -\ln\left(\frac{C_+^{right}}{C_+^{left}}\right) = \ln\left(\frac{C_-^{right}}{C_-^{left}}\right) \quad (5)$$

At the nanopore entrances, eq 5 can be written as the well-known Donnan potential drop, $\varphi'_D = \ln(C_>') = \sinh^{-1}(\Delta C'/2)$. To avoid confusion, we will use φ_D with its actual sign; that is, it will be $-\varphi_D$ inside a channel with negatively charged walls.

Linear combinations of ionic fluxes are often more convenient to deal with than individual fluxes. The PNP equation in the 1D approach is then written as

$$\begin{cases} J'_+ + J'_- = \alpha = -\dfrac{dC'}{dz} - \Delta C'\dfrac{d\varphi'}{dz} \\ J'_+ - J'_- = -J' = \dfrac{d\Delta C'}{dz} - C'\dfrac{d\varphi'}{dz} \end{cases} \quad (6)$$

where the fluxes J_i are normalized by the diffusion coefficient, $J_i' = J_i/D$. The total ionic current then equals $I = e\pi a^2 DJ'C_{bulk}$.

It is useful to define the ionic selectivity in a similar manner to that used for uniformly charged nanochannels:[34]

$$S = \frac{I_+ - I_-}{I_+ + I_-} = \left|\frac{\alpha}{J'}\right| \quad (7)$$

The selectivity is constant throughout the channel and defines a preference for particular ions to be transported. The total exclusion of one type of ion corresponds to $S = 1$, which describes a perfectly selective channel, while $S = 0$ describes a nonselective channel.

Channels with nonuniform surface charge distributions can demonstrate a significantly different current depending on the bias sign, that is, representing the ionic diodes. In order to describe such ionic diodes, we will use a similar analysis as the one shown in ref 34, that is, 3D numerical solution of PNP and analytical pseudo-1D approximations. Two extreme cases of ex-

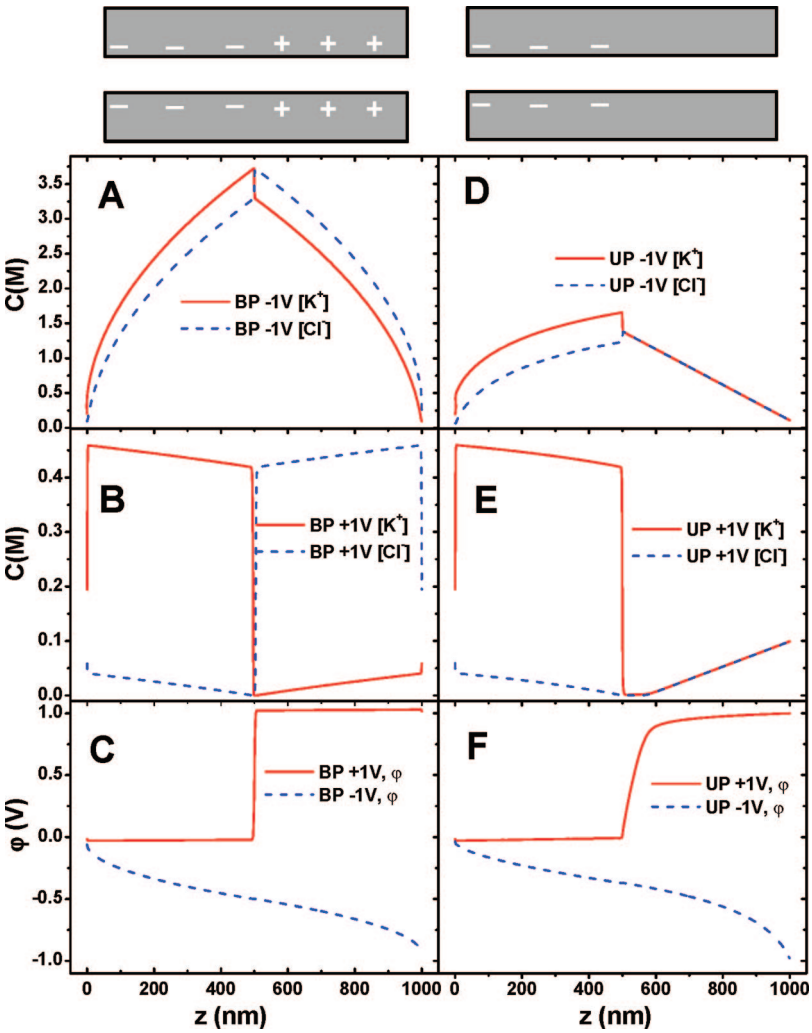

Figure 2. Profiles of the average ion concentrations and the electric potentials calculated for bipolar, BP (A−C), and unipolar, UP (D−F) diodes that were based on a 1 μm long nanochannel with $a = 4$ nm radius and $\sigma = 0.5e/nm^2$. The bulk KCl concentration is $C_{bulk} = 0.1$M. (A and D) Open-state (forward bias) concentrations of K^+ and Cl^-. (B and E) Concentration profiles of K^+ and Cl^- ions in the closed state (reverse bias). (C and F) Electric potential profiles for two biases.

perimentally realizable nanofluidic diodes will be investigated: bipolar diodes and unipolar diodes. A bipolar (BP) diode has two segments in the nanochannel with surface charges of the opposite sign and the same charge density: $-\sigma$ from 0 to z_0, and $+\sigma$, from z_0 to L (Figure 1). With no bias applied, the part of the pore with negative surface charges is cation selective, while in the other part (with positive surface charges), anions are the majority carriers. A unipolar (UP) diode is similarly formed with one part of the channel charged (either positively or negatively) and the other part neutral. We will consider a UP diode with negative surface charge density, $-\sigma$ from 0 to z_0, and neutral in the remaining portion, from z_0 to L. Thus, the negative bias on the right-hand side will be the forward bias (or an "open state" of the diode), while the positive bias on the right-hand side should correspond to the reverse bias (or the "closed state"). The parameter z_0 indicates the position of the transition zone, where the surface charge drastically changes. We will typically locate it at the center, $z_0 = L/2$. Intermediate situations, where the charge densities in the two zones of the pore are dissimilar in a different manner and/or the channel diameter changes along z, will also constitute a nanofluidic diode, but these systems will not be considered here.

RESULTS AND DISCUSSIONS

Figure 2 compares the ionic concentrations and electric potential profiles for BP and UP diodes for forward and reverse biases. The profiles were calculated by numerically solving the PNP equations (eq 2). As expected, the forward bias causes an enhancement of K^+ and Cl^- concentrations inside the pore, especially in the transition zone (Figure 2A,D), while the reverse bias produces very low ionic concentrations near $z = z_0$, effectively leading to the formation of a depletion zone (Figure 2B,E). At the reverse bias, almost the whole voltage drop occurs at the depletion zone (Figure 2C,F). The effect is more pronounced for a BP diode, which makes it a better diode.

The quality of an ionic diodes' performance can be described by the rectification factor, Q, calculated as the ratio of currents measured at opposite voltages of the same magnitude:

$$Q = \frac{I_{open}(V)}{I_{closed}(-V)} \qquad (8)$$

Higher values of $Q(V)$ correspond to better diode characteristics. The rectification factor for BP and UP diodes depends on the channel length, diameter, concentration of ions, and the bias voltage (Figures 3–7). The numerical calculations are compared with simplified 1D analyses based on eq 6, which we show separately for each type of diode.

Bipolar (BP) Diode. Because of the device symmetry, the value of $\alpha = J'_+ + J'_-$ (eq 6) for a BP diode equals 0, and ΔC can be taken as a constant (but of the opposite sign on each side of the diode). In the 1D approximation, the total concentration (*i.e.*, the sum $C_+ + C_-$ at z_0 should be continuous, while the potential should jump in accordance with eq 5. At the edges, the potentials jump by $-\varphi_D$ and $+\varphi_D$, respectively, with respect to the potential in the reservoirs, while the concentrations inside the pore should be equal to C_D at the both edges. The open state corresponds to the negative bias, $-V$, applied at the right reservoir.

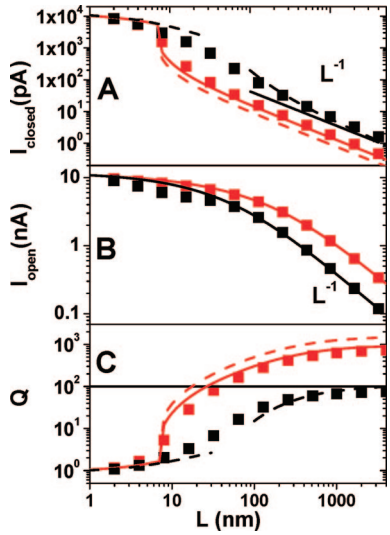

Figure 3. Transport properties of ionic diodes as a function of the nanochannel length. Numerical calculations (PNP) for UP (black) and BP (red) diodes with $a = 4$ nm, $z_0 = L/2$, $|\sigma| = 0.5$ e/nm^2, 1 V bias, and $C_{bulk} = 0.1$ M are compared with 1D approximations. (A) The current at reverse bias and its 1D approximations using: dashed red line (eq 12a) for $L > l_{dep} = 6$ nm combined with eq 29 for $L < 6$ nm; solid red line (eq 12a) scaled by a factor 1.6 (to match the PL approximation) for $L > 6$ nm combined with eq 29 for $L < 6$ nm; solid black line (eq 27a); dashed black line (eq 27) with C_{dep} from eq 24) and l_{dep} from eq 23) for $L > 100$ nm; shorter lengths ($L < 30$ nm) are described by eq 29. (B) Current for forward bias and its 1D approximations using: solid red line (eq 9); solid black line (eq 17). (C) Rectification factor and its approximation calculated using the above formulas. See text for details.

Substitution of $d\varphi'/dz = (1/\Delta C')dC'/dz$ from eq 6 (top) allows integration of eq 6 (bottom) to obtain $J'L = (C'_0{}^2 - C'_D{}^2)$, where C_0 is the concentration in the middle. The variation of the potential can be found by integrating eq 6 (*e.g.*, $\varphi'_L = -\varphi'_D - (C_0 - C'_D)/\Delta C'$) on the left-hand side. A similar integration on the right-hand side, in combination with the boundary conditions mentioned above, produces the following transcendental expression for the voltage−current ($V-I$) dependence:

$$V = \frac{2}{\Delta C'}\left(\sqrt{C_D'^2 + \Delta C' L J'} - C'_D\right) + 2\ln\frac{(\Delta C' + C'_D)}{2} + \ln\frac{\sqrt{C_D'^2 + \Delta C' L J'} - \Delta C'}{\sqrt{C_D'^2 + \Delta C' L J'} + \Delta C'} + J'\frac{\pi a}{4} \quad (9)$$

As the last term, we have also included the so-called Hall resistance, which is the access resistance at the channel edges for a neutral channel. This term can be neglected for long diodes but becomes important for short diodes and high biases. Since $\alpha = 0$ in the BP diode, assignment of the entrance resistance by Hall resistance should work well at least with neutral reservoir walls. The PNP calculations presented in Figure 3B appear to be in good agreement with eq 9 for the open state in long diodes.

In the limit of small bias ($V \ll k_BT/e$) in long diodes, eq 9 produces a linear $I-V$ dependence, but with the current only a quarter of the value found for a uniformly charged nanochannel:

$$I^{BP}_{open} \approx e^2\pi a^2 C_D \frac{D}{4k_BT}\frac{V}{L} \quad (10)$$

In the opposite limit, the square root of the current is a linear function of the bias

$$I^{BP}_{open} \approx \left(\frac{ea}{2k_BT}\right)^2 \frac{e\pi D\Delta C}{L}(V + V_0)^2 \quad (11)$$

where the intercept, $V_0 = 2k_BT/e\,(C_D/\Delta C - \ln((C_D + \Delta C)/2C_{bulk}))$, changes sign from positive to negative at $\Delta C/C_{bulk} = 3$. Formulas similar to eq 11 were obtained for BP membranes[35] and more recently for single channels,[11] but the value of V_0 was different. Figures 3and 4 clearly show that eq 9 agrees very well with the numerical PNP calculations for long diodes. Expression 9 is applicable for the reverse bias as well; one simply has to change the signs for the current and the bias. In the limit of small V, it reduces to the same (eq 10). High reverse bias, according to eq 12, produces current in the closed state that is independent of V:

$$I^{BP}_{closed} = 4e\pi D\frac{a^2C^2_{bulk}}{\Delta C L} = 2e^2\pi D\frac{a^3C^2_{bulk}}{\sigma L} \quad (12)$$

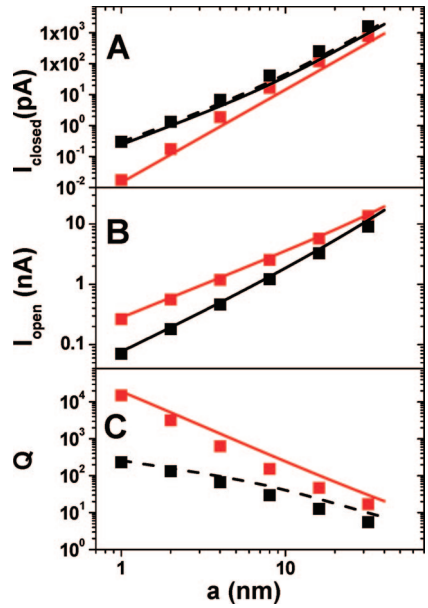

Figure 4. Transport properties of ionic diodes as a function of the nanochannel radius calculated for $L = 1$ μm, $|\sigma| = 0.5$ e/nm^2, $z_0 = L/2$, 1 V bias, and $C_{bulk} = 0.1$ M. Numerical (PNP) calculations for UP (black) and BP (red) diodes are compared with 1D approximations. (A) Current at reverse bias; solid red line, 1D estimate using eq 12; solid black line (eq 27a); dashed black line (eq 27) with C_{dep} from eq 24. (B) Current at forward bias: solid red line (eq 9); black solid line (eq 19). (C) Rectification factor and its approximation calculated using the above formulas. See text for details.

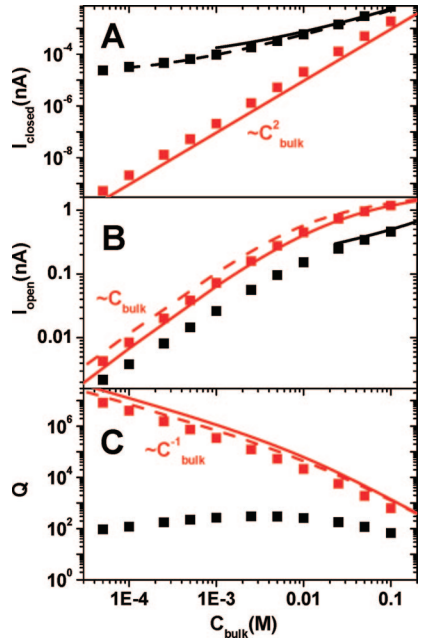

Figure 5. Transport properties of ionic diodes as a function of the ionic concentration, C_{bulk}, calculated numerically (PNP) for $L = 1$ μm, $|\sigma| = 0.5$ e/nm^2, $z_0 = L/2$, 1 V bias, and $a = 4$ nm. Numerical (3D PNP) calculations for UP (black) and BP (red) diodes are compared with 1D approximations. (A) Current at reverse bias and its 1D approximations using: solid red line (eq 12); solid black line (eq 27), with C_{dep} from eq 25; dashed black line (eq 27), with C_{dep} from eq 24. (B) Current at forward bias; solid red line (eq 9) and dashed red line (eq 11); solid black line (eq 19). (C) Rectification factor and its approximation calculated using the above formulas. See text for details.

From graphical analysis, the transition from eq 10 to eq 12 occurs at a bias of $V \sim 3k_BT/e$. The current in the closed state in BP diodes is reasonably well explained by eq 12: both the characteristic cubic dependence on the pore radius (Figure 4) and quadratic dependence on the bulk ion concentration (Figure 5) are clearly visible. The absolute value of the current in the closed state is, however, underestimated by eq 12 by approximately a factor of 2 (see Figure 5). The poorer accuracy of the closed-state description is due to the shortcomings of the 1D Donnan equilibrium treatment in predicting the minority carrier concentration in nanopores. The PL approximation of PB does a better job and is only 20% below that of numerically obtained PNP values.

Minority carriers are responsible for the current in the closed state, which is clear from the alternative derivation of eq 12, similar to that used in semiconductor p−n junction diodes. The electric field under reverse bias is very small everywhere except for the depletion zone. In long diodes, the depletion zone is so short that it can be neglected and thus one can assume that the electric field, $d\varphi/dz$, is zero everywhere. At the same time, the ionic concentrations are low, especially near the depletion zone, which suggests that the contribution of ion drift in the field to the total flux is negligible. The fluxes of each ion should not depend on z; therefore, one can calculate their values at any z, for example, at the portion where each ion becomes a minority carrier. The assumption that $d\varphi/dz = 0$ suggests that the K^+ concentration drops linearly from the equilibrium concentration $C_+(L)$ at the right pore entrance ($z = L$) to zero at $z = z_0$. This implies that the concentration of potassium ions is given by $C_+(z) = C_+(L)\ (z - z_0)/(L - z_0)$ for $z_0 < z < L$ (Figure 2B), while the concentration of chloride changes as $C_-(z) = C_-(0)\ (z_0 - z)/z_0$ for $0 < z < z_0$. Both $C_+(L)$ and $C_-(0)$ are the same and equal $C_<$ as given by eq 4. The total ionic current at a reverse bias for a BP diode can be then estimated as:

$$I^{BP}_{closed} = eD\pi a^2\left[\left(\frac{dC_+}{dz}\right)_{right} - \left(\frac{dC_-}{dz}\right)_{left}\right] = eD\pi a^2 C_< \frac{L}{z_0(L - z_0)} \quad (13)$$

which reduces to eq 12 after substituting $C_<$ from eq 4 in the limit of high surface charge densities, and $z_0 = L/2$. Note that the reverse current has a minimum value for $z_0 = L/2$; that is, an (anti)symmetric BP diode would have the minimal reverse current (see details in Supporting Information).

The quadratic voltage dependence of the current in the open state from eq 11 cannot last long; it becomes linear due to the substantial voltage drop at the diode entrances when the voltage drop across the diode channel reaches the value of the voltage drop across the Hall resistance, that is, at the critical bias:

$$V^{BP}_c \sim \frac{8LC_{bulk}}{\pi}\frac{k_BT}{\sigma} \quad (14)$$

This critical bias is similar to the value found for a homogeneously charged nanochannel of the same surface charge density and length.[34] For a diode with $\sigma = 0.5$e/nm^2, the condition of eq 14 at 1 V is realized for quite long diodes, $L \sim 200$ nm; a departure from the quadratic dependence of the open-state current on voltage appears noticeable even at lower voltages. One can reveal V_c^{BP} by monitoring the diode current at a constant bias for channels of different values of L or by changing the ion concentration. Figures 3 and 4 illustrate an exceptionally good agreement between the numerical PNP calculations and the corresponding 1D modeling using eq 9 for long diodes. A departure from the simple dependence given by eq 11 is clearly visible even for 1 μm long diodes in $C_{bulk} = 0.1$ M.

The current in the closed state of a BP diode is also sensitive to its length, but the physics of this dependence is different. Figure 3 illustrates that the simple $1/L$ dependence in eq 12 is observed down to channels as short as 10 nm, at least for 1 V bias. The reason for the departure from this simple behavior is not the access resistance, but rather the width of the depletion zone, l_{dep}, becoming comparable to the overall device

length L. The depletion zone forms between the two oppositely charged segments of the pore. It can appear as a transition zone during construction of the diode, but even in a perfectly abrupt transition, it widens upon increasing the reverse bias. In order to explain this effect, one has to repeal the simplification of the Laplace equation that we have employed in our 1D description and consider the Poisson equation, $d^2\varphi'/dz^2 = -k^2\Delta C'$ in the vicinity of the separation zone. This analysis is analogous to the approach used for the semiconductor PN junction.[36] In a simple approximation, one can assume ΔC to be constant with opposite signs on the two sides of the depletion zone. The resulting potential changes quadratically with the distance in both directions away from the center and reaches the limiting values within $l_{dep}/2$ on each side, where

$$l_{dep} \approx 2\sqrt{\frac{V'}{k^2\Delta C'}} = \sqrt{\frac{2V\varepsilon\varepsilon_0}{e\Delta C}} = \sqrt{\frac{Va\varepsilon\varepsilon_0}{\sigma}} \qquad (15)$$

Note that the width of the depletion zone appears independent of the diode's length and the bulk ion concentration but increases with the pore radius and bias. The width becomes comparable to the pore diameter at relatively low biases: for example, at 1 V, $l_{dep} \sim 6$ nm for $a = 4$ nm and $\sigma = 0.5$e/nm^2. The diode "opens up" at the reverse bias when the depletion zone extends to the full length of the diode, at which point, the diode's performance can be approximated as a neutral pore (see eq 23 in ref 34). We would like to emphasize that the diode opening up effect shown here has a very different physical basis than the dramatic increase of the reverse currents shown for bipolar membranes,[8,9] where it occurred due to presumed dissociation of water.

The current for short diodes but with $L > l_{dep}$ is also affected by the depletion zone length. One can accommodate this fact by recalling how eq 13 was derived. The region where the potential gradient is zero now extends over $L - l_{dep}$, rather than over the whole L, thus the current can be rescaled as

$$I^{BP}_{closed} = 2e^2\pi D\frac{a^3C^2_{bulk}}{\sigma(L - l_{dep})} \qquad (12a)$$

where l_{dep} is given by eq 15. Obviously, the contribution of l_{dep} becomes undistinguishable when L increases. Equation 12a indeed describes very well the variation of the current in the closed state with channel lengths down to l_{dep}, as Figure 3 illustrates. For shorter diodes, the depletion zone extends over the whole diode length, which resembles the situation of a neutral channel, and consequently, the current can be described by the equation derived for a neutral pore (eq 23 in ref 34). Given the simplicity of our description of the depletion zone, the agreement between the 1D approximation and the numerical PNP calculations appears surprisingly good.

The rectification factor, Q, calculated from eq 8 using the above-described approximations of the currents for forward and reverse biases, also shows remarkably good agreement with the numerical PNP predictions. Not only does it correctly capture the a^{-2} dependence of Q on the radius (Figure 4), and the pseudo-$1/C_{bulk}$ dependence on the electrolyte concentration (Figure 5) but it also very nicely reproduces the more complicated dependence on the diode length (Figure 3).

Interestingly, the diode would demonstrate the "closed" state and the corresponding rectifying behavior even for short pores having lengths smaller than their diameter, provided that the bias is not large. The minimal length for which no current rectification occurs can be estimated by substituting $l_{dep} = L$ in eq 12, and the minimum voltage, $V \sim k_BT/e$ for which the saturation of the reverse current can be still achieved in accordance with eq 12. The resulting condition

$$L_{min} = \sqrt{\frac{k_BT}{e}\frac{a\varepsilon\varepsilon_0}{\sigma}} \qquad (16)$$

defines the minimum length for a diode. Note that the aspect ratio, a/L, does not represent a good scaling parameter; more appropriate is the ratio a/L^2. Equation 16 also suggests that some ion current rectification can be observed even for L as short as 2 nm when a diode is based on a nanopore with $a = 4$ nm and $\sigma = 0.5$e/nm^2, and the bias does not exceed ~0.1 V. As it was already pointed out above, this critical diode length is independent of the bulk ion concentration and is optimal (*i.e.*, resulting in the highest Q) for an antisymmetric configuration, that is, when the lengths of positively and negatively charged segments are identical. Figure 6compares the $I-V$ curves that were calculated numerically (3D PNP) with the 1D approximation curve obtained from eq 9. The correspondence between the numerical and the analytical solutions is very good.

Current−voltage ($I-V$) dependences for very short BP diodes are shown in Figure 7A. Diodes with very low aspect ratios (*e.g.*, with $L = 2$ nm and $a = 4$ nm) show almost no rectification. The resistance in this case approaches the Hall resistance. Longer devices, however, have the characteristic low currents under reverse bias, which disappear at higher voltages. As eq 15 states, longer diodes require higher biases for opening up.

When nanofluidic diodes are short, the reservoir walls that are in contact with the pore entrances play a significant role in determination of transport properties of the devices. Similar to the charged nanochannel case,[34] ionic currents for nanofluidic diodes are higher for the open state and lower for the closed state when the reservoir walls have the same charge density as the

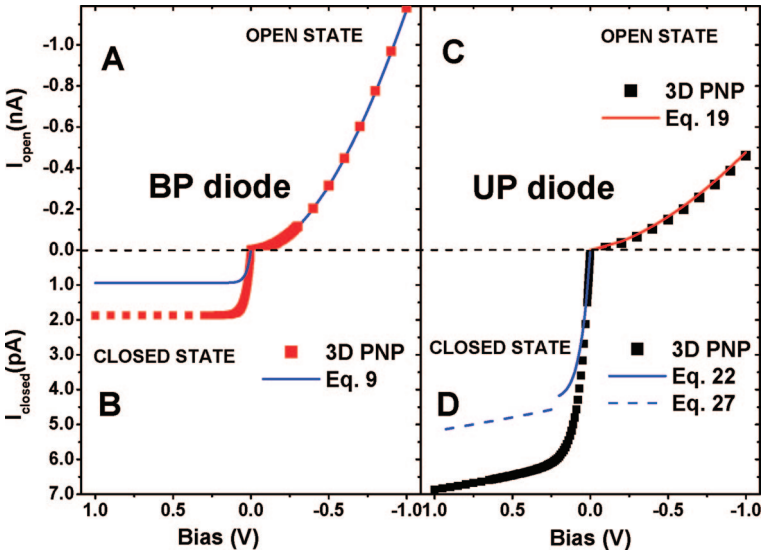

Figure 6. Current−voltage ($I-V$) dependences of a BP (A, B) and a UP (C, D) diodes with $L = 1$ μm, $a = 4$ nm, $z_0 = L/2$, $C_{bulk} = 0.1$ M, and $\sigma = 0.5e/nm^2$. Points (red and black) are calculated numerically using 3D PNP. (A) Open state of a BP diode. Blue curve shows the results of eq 9. (B) Closed state. The calculated current from eq 9 shows lower current values due to the underestimation of the minority carrier concentrations by the Donnan approximation (the PL approximation gives better quantitative agreement). (C) Open state of a UP diode. The red curve shows the results of eq 19. (D) Closed state: for bias < 0.25 V, the depletion zone is not formed and the current is described by eq 22; the situation with biases larger than 0.25 V is described by eq 27. Note different scales for open and closed states.

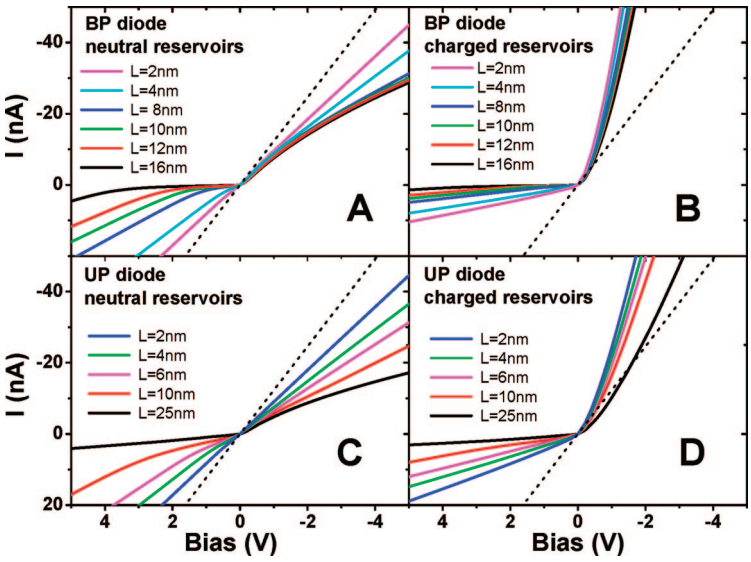

Figure 7. Current−voltage ($I-V$) dependences calculated numerically using 3D PNP for diodes with $a = 4$ nm, $\sigma = 0.5e/nm^2$, $C_{bulk} = 0.1$ M, and various (small) lengths. (A) BP diodes with neutral reservoir walls: even devices with low aspect ratios show rectification at small biases. The longer the diode, the higher the biases at which the diode opens up. The minimum diode length that assures ion current rectification can be estimated using eq 15. The resistance is always greater than Hall resistance (dashed line). (B) BP diodes with the reservoir walls having the same surface charge density as the corresponding sides of the channel. (C) UP diodes with neutral reservoir walls: Longer lengths are necessary to observe noticeable rectification. Equation 30 allows the estimation of the minimal diode length. (D) UP diodes with reservoir walls having the same surface charge density as the corresponding sides of the channel.

corresponding side of the nanochannel (see Figure 7B). Thus charging the reservoir walls significantly improves the devices' performance. It is the effective "preconditioning" of the concentrations at the nanochannel edges in this case that reduces the entrance resistance and the polarization effects. As Figure 7B illustrates, even ultrashort diodes of only 1 nm long demonstrate remarkable rectification characteristics. Moreover, no breaking down (opening) is observed at reverse biases up to 5 V, and the open-state resistance is smaller than the Hall resistance. For the parameters of Figure 7, the open-state resistance is nearly three times smaller than the Hall resistance, which indicates a significant segregation of ions of opposite charges near the edges. Obviously, our 1D approximation is not applicable for evaluation of such very short diodes, for which a full 3D analysis would have to be performed. The effect of charged reservoir walls diminishes in long diodes, where the diode resistance becomes the limiting factor (see details in Supporting Information). In the ultrashort diodes, on the other hand, the distribution of charges inside the channel becomes unimportant as the diode's performance is dictated by the reservoir walls; the $I-V$ curves barely change if the nanochannel surface is set to have zero charge (see Supporting Information for details).

Summary of the Analysis of a Bipolar Diode (BP). A BP diode has maximum rectification when the two oppositely charged segments have an equal length. Equation 9 gives a good quantitative description of the $I-V$ curve of a BP diode for all biases. At large reverse biases, a BP diode shows current that is independent of the bias, a property that is similar to the semiconductor PN junction. The value of the reverse current is underestimated by *ca.* a factor of 2 in eqs 9, 12, and 13, but better approximations for the minority carrier concentrations (*e.g.*, PL[33]) provide almost a perfect quantitative agreement. Upon further increase of the reverse bias, the depletion zone grows in width (proportional to $\sim V^{1/2}$) and can reach the length of the diode, which has been taken into account *via* eq 15. The rectification factor is the highest for long diodes, when currents for both forward and reverse biases decline linearly with length, $\sim L^{-1}$, and the diode resistance is dominant. The forward and reverse currents have a^1 and a^3 dependences on radii, respectively, making the rectification factor proportional to a^{-2}. Dependence on the bulk ionic concentration is quadratic, C_{bulk}^2, for the open-state current, and linear, C_{bulk}, for the closed-state current, yielding the C_{bulk}^{-1} dependence of the rectification factor. The rectification effect decreases strongly for very short diodes containing neutral reservoir walls.

Noticeable rectification is, however, observed for even very short diodes of aspect ratio equal to one or less when the reservoirs are charged as well (eq 16).

Unipolar (UP) Diode. The case of the unipolar (UP) diode is more complicated than that of the BP because of the low symmetry of the device. The ion fluxes, J_+ and J_-, are no longer equal and the electroneutrality condition that we employed for the 1D approximation in PB is not fulfilled in many regions of UP diode. Strictly speaking, in this case, one has to solve the Poisson equation. Nevertheless, at forward bias, the current is high enough and the selectivity is correspondingly low, making the treatment using the Laplace equation satisfactory.

Under this approximation, we can apply a treatment similar to the approach used for the BP diode (see details in Supporting Information). There are four sections of the diode on which the applied potential drops: the entrance into the charged section, the charged segment, the neutral channel, and the intersection between the charged and neutral segments (with $\Delta\varphi_C$). The sum of these potentials equals the applied bias. We will presume that $C(z_0) = C_0$ is continuous and calculate the corresponding jump in the potential $\Delta\varphi_C$.

The value of α in eq 6 is no longer zero but equals the negative gradient of the total concentration in the neutral part (*i.e.*, for $z_0 = L/2$, it is $\alpha = 2(C_0' - 2)/L$. The concentrations and the potential drops on each section can be expressed through C_0. The latter can be found by integrating eq 6:

$$C_0' = \frac{1}{3}(2 + \sqrt{(4 + 3C_D'^2 - 3\Delta C' JL)}$$

The overall equation for the voltage−current dependence becomes

$$V' = -\sinh\left(\frac{\Delta C'}{2}\right) - \ln\left(\frac{C_0'}{C_0' + \Delta C'}\right) + \frac{J'L}{2(C_0' - 2)}\ln\left(\frac{C_0'}{2}\right) + \frac{1}{\Delta C'}(C_D' - 2(C_0' - 1)) + J'\frac{\pi a}{4} \quad (17)$$

The first term of eq 17 is the Donnan potential, $-\varphi_D$, the second is the potential jump $\Delta\varphi_C$ at $z = z_0$, and the third and the forth terms are potential drops on the neutral, $\Delta\varphi_R$, and the charged, $\Delta\varphi_L$, segments, respectively. The contribution from the entrance resistance is also included as the Hall resistance in the last term.

By presuming that $C(z_0) \gg C_D$ and neglecting φ_D, eq 17 in the limit of long diodes can be simplified to a transcendental formula for the current:

$$J' = -\frac{\frac{3\Delta C'}{4L}V'^2}{\left[1 + \frac{3}{8}\ln\left(\frac{\Delta C'|J'|L}{3}\right)\right]^2} \quad (18)$$

Iteration $J_{n+1}' = F(J_n')$ with the initial step ($n = 0$) $J_0' = -3\Delta C'/4LV'^2$ allows its further simplification:

$$I_{open}^{UP} = -e\frac{\pi^2 a^2}{2}\frac{\frac{3D\Delta C}{4L}\left(\frac{eV}{k_BT}\right)^2}{\left[1 + \frac{3}{4}\ln\left(-\frac{\Delta CeV}{4k_BTC_{bulk}}\right)\right]^2} \quad (19)$$

representing the current as an explicit function of bias. Note that the iteration beyond $n = 0$ results only in an additional coefficient close to $\pi/2$ (shown in Supporting Information). Neither eq 17 nor eq 19 provides a correct current behavior at small biases or at a reverse bias. This is not surprising since in the closed state of this diode we have to solve the Poisson equation. Nevertheless, as Figures 3 and 4 demonstrate, the value of forward currents in long diodes at 1 V bias is explained relatively well by eq 19. Both the pore radius dependence ($\sim 1/a^{3/2}$) and the inverse dependence on the diode length are well reproduced. Upon shortening the diode length, the pseudo-quadratic dependence of the current on voltage of eq 19 saturates. For short UP diodes, even with the Hall resistance included, eq 17 overestimates the current because of the additional concentration drop at the charged nanochannel entrance, which results in an extra voltage drop (polarization) at that entrance (see eq 20 and Figure 6A of ref 34).

Although the dependence of I^{UP}_{open} on C_{bulk} is weak (supralinear) and hidden in eq 19, it is still reasonably well reproduced at high concentrations (see Figure 5B). For small ionic strengths ($ka \sim 1$), eq 19 fails because of a significant discontinuity of $C(z_0)$ at the point where the surface charge changes from σ to 0 (Figure 5B).

Equation 19 describes the $I-V$ curve for a UP diode in the open state quite well (see Figure 7C). Slight overestimation of the current is due to neglecting φ_D and not taking into account the concentration polarization at the charged segment entrance. The case of the UP diode under reverse bias will be considered separately for low and moderate biases.

UP Diode under Low Reverse Bias. The ion selectivity of a BP diode is zero because the device is fully symmetric. A UP diode is not as symmetric, and S should be nonzero; a nonselective UP diode ($S = 0$) would not rectify the ion current. We presume that the charged segment at a low bias behaves in a similar way to a homogeneously charged nanochannel (*i.e.*, the sum of all charges is zero throughout). Again, one can identify four sections of the diode on which the applied potential drops, and they can be expressed through C_0, the ion concentration at $z = z_0 = L/2$:

$$-\varphi_D' + \frac{2 - C_0'}{\Delta C'} + \ln\left(\frac{2C_>'}{C_0'}\right) + \frac{1}{S}\ln\left(\frac{2}{C_0'}\right) = V' \quad (20)$$

The equation can be simplified by recognizing that the potential drop across the charged part of the di-

ode (the second term) is small (see Figure 2F) and thus can be neglected if $\Delta C \gg C_{bulk}$. Then C_0 can be found, which in a highly charged nanochannel with $S \approx 1$

$$C_0' = \sqrt{\frac{4C_>'}{\exp(V' + \varphi_D')}} \tag{21}$$

This concentration, therefore, very quickly declines with the bias and eventually a zone of low ion concentration, that is, the depletion zone is formed (see Figure 2F). The ionic current can be calculated on the basis of the charged segment, where the ion flow occurs primarily due to electromigration (*i.e.*, the ionic flux equals $J' = C'(d\varphi'/dz) = 1/S(dC'/dz)$). Thus, the current can be calculated using C_0 as

$$I^{UP}_{closed\_low} = \frac{2e\pi a^2 D}{S}\frac{(2C_{bulk} - C_0)}{L} \tag{22}$$

UP Diode under Moderate Reverse Bias. As seen from eq 21, C_0 decreases with the bias and eventually saturates at a very small value, C_{dep}, for $V \gg \varphi_D$. The C_0 decrease is accompanied by a widening of the region with small C_{dep}, which is referred to as the depletion zone, similar to that in a BP diode. The difference between a UP diode compared to a BP one is that the depletion zone is now confined almost exclusively to the neutral segment and its width is significantly greater than in a BP diode. As we mentioned above, the Laplace treatment of the depletion zone is not sufficient, and one has to solve the Poisson equation. The overall treatment of this case is similar to the description of the Schottky diode:[37] the charged segment of the nanopore corresponds to the metal part and the uncharged segment to the semiconductor part. By presuming that the ionic concentration inside the depletion zone is constant, C_{dep}, (which also means the difference between the concentrations of two ions, is constant $\delta C = SC_{dep}$) one can solve the Poisson equation, $\Delta\varphi'(z) = -k^2\delta C'$, to find the depletion zone width, l_{dep}:

$$l_{dep} = \sqrt{\frac{2V'}{Sk^2C_{dep}'}} \tag{23}$$

The value of C_{dep} can be estimated by realizing that the ion flux, which inside the depletion zone occurs primarily due to the electromigration, is equal to the flux through the uncharged segment, where the ions diffuse due to the concentration gradient (the electric field there is close to zero). The resulting expression for balancing the flux in the two zones becomes

$$k^2\frac{SC_{dep}'^2 l_{dep}}{2} = \frac{1}{S}\frac{2 - C_{dep}'}{L/2 - l_{dep}} \tag{24}$$

After substituting l_{dep} from eq 23, in the limit of $L/2 \gg l_{dep}$, one obtains the concentration in the depletion zone as

$$C_{dep}' = \frac{2}{S}\left(\frac{4}{k^2V'L^2}\right)^{1/3} \tag{25}$$

This formula leads to the expression for the depletion zone width

$$l_{dep} = \left(\frac{LV'^2}{2k^2}\right)^{1/3} \tag{26}$$

which is in a good agreement with numerical calculations (see details in Supporting Information).

Note that l_{dep} from eq 26 depends not only on the bias but, in contrast to BP diode, also on L and the bulk ion concentration, C_{bulk}. On the other hand, it does not depend on the nanochannel radius or the charge density of the charged segment. This is understandable since the depletion zone is confined to the uncharged segment, at least in cases when the selectivity of the charged segment is significant. The situation with low S in the charged segment is not covered by eq 26, but for large S, eq 26 is in a good agreement with numerical 3D PNP analysis: the 2/3 power dependence on the bias, the 1/3 power dependence on L, and the $-1/3$ power on C_{bulk} are very well reproduced. Equation 26 slightly overestimates the depletion zone width compared to the numerical calculations. For example, for $L = 1$ μm, 1 V bias, and $C_{bulk} = 0.1$M, eq 26 yields $l_{dep} \sim 90$ nm, while the 3D PNP numerical solution gives $l_{dep} \sim 80$ nm. The discrepancy is surprisingly small (<15%) taking into account the set of approximations that were made: constant C_{dep} throughout the depletion zone, constant electric field inside that zone, and zero electric field in the remaining part of the uncharged segment.

The resulting expression for the current in a UP diode under moderate reverse bias is given by

$$I^{UP}_{closed\_med} = \frac{2e\pi a^2 D}{S}\frac{(2C_{bulk} - C_{dep})}{L - 2l_{dep}} = k^2\frac{Se\pi a^2 D l_{dep}C_{dep}^2}{2C_{bulk}^2} \tag{27}$$

where l_{dep} is defined by eq 26 and C_{dep} – by eq 25. Equation 27 transforms into eq 22 at low reverse bias, when l_{dep} is zero, and the concentration in the depletion zone is replaced by C_0 from eq 21. Despite its simplicity, eq 27 catches the correct dependence of $I^{UP}_{closed\_med}$ on L and a (Figures 3 and 4). There is a range of high enough biases in long diodes when the depletion zone is formed, $C_{bulk} \gg C_{dep}$, but its length is much smaller than $L/2$ and can be neglected. Then eq 27 simplifies to

$$I^{UP}_{closed\_med} = \frac{4e\pi a^2 DC_{bulk}}{L}\frac{C_D}{\Delta C} \tag{27a}$$

with the current independent of the applied voltage, similar to the closed state in BP diodes. In UP diodes, this current is higher than in BP diodes by a factor of C_D/C_{bulk}. As seen from Figure 3A, this factor $C_D/C_{bulk} \sim 4$ holds nicely for diodes with $L > 1000$ nm.

UP Diode under High Reverse Bias. Equation 27 fails at large biases when l_{dep} reaches $L/2$ and one has to solve the Poisson equation for the whole neutral segment. Similar shortcomings in the current dependence on C_{bulk} can be traced. Equation 27 describes the dependence of $I^{UP}_{closed\_med}$ on C_{bulk} for moderate ionic strengths fairly well (Figure 5A); the dependence is close to linear when the contributions of C_{dep} and l_{dep} are small. In this case, the C_{dep} and l_{dep} contributions partially cancel each other. At small C_{bulk} and/or large bias, when l_{dep} expands toward $L/2$, a different expression for C_{dep} arises:

$$C'_{dep} = \frac{8V'}{Sk^2L^2} \tag{28}$$

Note that now (when the depletion zone covers the whole neutral region) C_{dep} starts *increasing* with the bias. The expression of eq 27 is still applicable with the new meaning of C_{dep} and l_{dep} and results in a strong increase of the current with bias ($\sim V^2$) and/or shortening of the channel ($\sim L^{-3}$). Because of the fast current rise, the range of biases/lengths where the corresponding dependence can be observed is very narrow and barely recognizable for short diodes. However, at longer lengths, for example for $L = 1$ μm, the V^2 dependence of the current is clearly visible. As soon as C_{dep} reaches $2C_{bulk}$, the diode ceases to rectify and the current becomes linearly dependent on the C_{bulk} and the bias:

$$I_{terminal} = \frac{V}{R} = \frac{2e^2DC_{bulk}a}{k_BT\left(\frac{L}{\pi a} + \frac{1}{2}\right)}V \tag{29}$$

Equation 29 is analogous to eq 23 from ref 34, describing the current through a neutral channel. Transition to this terminal dependence is difficult to describe analytically in detail for UP diode. That is why merely merging it with eq 27 for short lengths does not fit the overall I^{UP}_{closed} dependence on L well (see Figure 3). In the case of BP diodes, on the other hand, application of eq 29 works better.

The dependence of l_{dep} on C_{bulk} is the reason for the existence of the rectification factor, Q, maximum at concentrations for which $L/2 \sim l_{dep}$ (Figure 5C). One has to note that, even though I^{UP}_{closed} at very low C_{bulk} follows eq 29, its interpretation in that case is different. When S is close to unity, at very low C_{bulk}, the whole neutral segment also becomes primarily filled with the majority carriers of concentration C_{bulk} (the minority carriers are expelled). This disparity of concentrations is accompanied by the applied voltage V dropping exclusively on the neutral segment. Thus, the ionic current can be estimated as due to electromigration of C_{bulk} in the field $2V/L$, which has the appearance of eq 29 and is confirmed by the numerical analysis (shown in Supporting Information). The rectification ratio decrease with C_{bulk} has recently been observed for a UP diode.[4] Conically shaped nanopores with homogeneous surface charges, which can also be considered similar to UP diodes, show analogous decrease in rectification.[5]

Figure 6C,D demonstrates an $I-V$ curve calculated for a UP diode. The reverse bias situation was calculated using eqs 22 and 27. The two equations describe relatively well both the shape and the magnitude of the current. Comparison of eqs 21 and 25 allows one to estimate the bias needed for the development of the depletion zone and for the transition to a weak variation of current:

$$\frac{\exp(V')}{V'^{2/3}} > \Delta C' \left(\frac{kL}{2}\right)^{\frac{4}{3}} \tag{30}$$

Obviously, this condition is affected by the surface charge and the pore radius as well as by the length ($\sim L^{4/3}$) and the ion concentration ($\sim C_{bulk}^{2/3}$). For the nanochannel considered in Figure 8, it corresponds to $V \sim 10\ k_BT/e$, or $V \sim 0.25$ V, which agrees well with the PNP calculations.

Some rectification will occur even when the depletion zone is not "well developed", that is, when C_0 in eq 21 is lower than C_{bulk}. In order to estimate the shortest UP diode length, let us set $C'_0 \sim 1$ (the concentration of each ion is half of that in the bulk). Then for a highly charged surface ($S \sim 1$, $C_> \sim \Delta C$), the minimum bias required for rectification from eq 21 is $V_{min}' > \ln(4\Delta C')$ or $V_{min} > 4k_BT/e$ using the same parameters as above ($a = 4$ nm, $C_{bulk} = 0.1$ M, and $\sigma = -0.5$e/nm^2). Since l_{dep} is longer in UP diodes than in BP diodes, UP diodes are more restricted toward miniaturization. The condition for the minimal length depends on many parameters identified in eqs 26, 28, and 30. The latter provides the low limit for the bias. The upper limit can be obtained from eq 28 by setting the maximum C_{dep} equal $2C_{bulk}$ when the diode ceases to rectify, that is, $V'_{max} < Sk^2L^2/4$. Convergence of the two limits crudely identifies the minimal UP diode length (with neutral reservoir walls):

$$L^{UP}_{min} > \frac{4}{\sqrt{S}k} \tag{31}$$

For example, for $C_{bulk} = 0.1$ M, $a = 4$ nm, and $\sigma = 0.5$e/nm^2, the minimal length according to eq 30 is $L^{UP}_{min} > 4$ nm. Such a short device is supposed to rectify the current only at low enough biases, ~0.1 V. This is a very crude estimate and does not provide the full physical picture. Numerical 3D PNP calculations demonstrate rectification for such short diodes but in a broader range of biases (Figure 7C). Nevertheless, this analysis

confirms that the size reduction in rectifying ionic devices can be achieved easier with BP diodes rather than with UP diodes. Not only is the rectification factor lower for UP diodes of the same length as BP diode, but the minimum length in UP diodes is also longer and increases with decreasing C_{bulk} (see eq 31). The minimum BP diode length L_{min}^{BP} does not show such a dependence (see eq 16).

Similar to a BP diode, a charged reservoir wall that is in contact with the entrance into the charged segment of the diode significantly improves the performance of very short UP diodes to outperform the estimate of eq 31. Again, the ionic currents in this case are higher for the open state and lower for the closed state (see Figure 7D) compared to the situation of a device with both neutral reservoir walls. UP diodes with charged reservoir walls also do not open at reverse biases up to 5 V, but the current at reverse bias is greater than that of similar BP diodes.

Summary of the Analysis of a Unipolar Diode. The absence of symmetry in this device makes approximate analytical solutions for a UP diode less convenient and requires individual considerations for different conditions. At moderate biases, current in the open state has pseudo-V^2 dependence (eq 19), but at higher bias and/or small diode lengths, it transforms into a linear dependence because of polarization effects. In long diodes, the current has L^{-1} dependence, similar to that in BP diodes. The treatment under reverse bias is analogous to that of a Schottky diode, where now the depletion zone width depends not only on bias ($\sim V^{2/3}$) but also on the channel length ($\sim L^{1/3}$), and the bulk ion concentration ($\sim C_{bulk}^{-1/3}$), as shown in eq 26. The depletion zone in a UP diode is much longer than in a BP diode of similar dimensions and extends primarily into the neutral segment. For larger reverse biases, the $I-V$ curve is well described by eq 27, which produces a weaker dependence of the closed-state current on the radius ($\sim a^{3/2}$) than the current in the open state ($\sim a^{5/2}$). Thus the rectification factor is proportional to a. At very large reverse biases and/or at low C_{bulk}, the depletion zone extends beyond the neutral segment and changes the current to a terminal current proportional to C_{bulk} (eq 29). Charging the reservoir wall on the charged side of the pore significantly improves the performance of very short diodes.

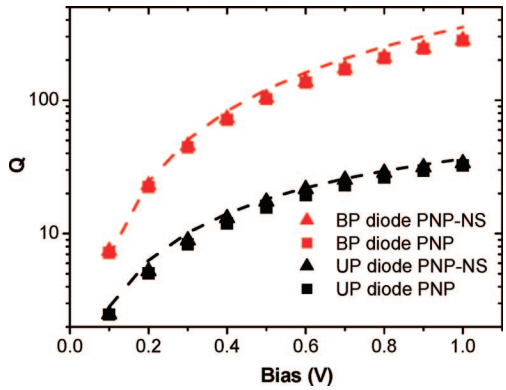

Figure 8. Evaluation of the electroosmosis effect on the rectification factor for diodes with $L = 128$ nm, $a = 4$ nm, $\sigma = 0.5e/nm^2$, and C_{bulk}=0.1 M with neutral reservoir walls. The rectification factor was numerically calculated for BP diodes using 3D PNP (red square) and 3D PNP-NS (red triangle). Similar calculations were performed for UP diodes: (black square) 3D PNP and (black triangle) 3D PNP-NS, respectively. The dashed lines demonstrate analytical 1D PNP approximations.

Contribution From Electroosmosis. Evaluation of the electroosmosis contribution to the ionic current requires solving the PNP-NS given by eq 1. The analytical solution of the PNP-NS equations for nanofluidic diodes is complicated (if ever possible). Thus, we performed only numerical analysis in this case. In nanochannels with homogeneous surface charges, the contribution of electroosmosis can be substantial[34] because the majority of carriers drift in the external electric field causing the solution as a whole to move along as well. In BP diodes, the surface charge changes sign at z_0 and the overall solution velocity through the device should be close to zero. Even for quite short diodes with $L = 128$ nm, one can see only a minor change in the rectification factor as obtained from PNP-NS compared to the PNP treatment (Figure 8). Solution of PNP-NS for a UP diode also shows only a small deviation from the PNP treatment. Here the neutral segment of the channel limits the electroosmotic contribution.

CONCLUSIONS

The modeling of nanofluidic diodes presented here has been inspired by recent experimental realization of these devices.[4,5,27] Studies of ion transport through nanofluidic diodes performed thus far have been mostly focused on the dependence of their lateral dimension (*e.g.*, diameter).[11] Much less attention has been paid to the influence of the longitudinal dimension on the diodes' functioning. The ability to shorten the diodes while retaining their rectifying capabilities is very important in applying them as components of ionic circuits, artificial cells, and laboratory-on-the chip systems. We also feel that, in order to make the rectifying systems accessible to a wide scientific audience, it is important to provide suitable analytical formulas describing the diodes' properties. Such formulas should allow one to perform very convenient "back-of-the-envelope" calculations, which will give the diameter, length, and surface charge distribution of a device necessary to obtain required diode characteristics.

In this paper, we have provided a thorough analysis of the ionic currents through nanofluidic diodes and how the currents depend on the channel length and radius, surface charge density distribution, the applied voltage, as well as the ionic strength of the bulk solution. Two types of diodes, bipolar and unipolar, have been compared, and their functioning was found to be similar to a p–n semiconductor junction and a solid-

state Schottky diode for a bipolar diode and a unipolar diode, respectively.

We have demonstrated that the contribution of electroosmosis for both types of diodes (bipolar and unipolar) is usually negligible and the devices can be described using the PNP system (eq 2), rather than the complete description involving PNP-NS (eq 1). The full 3D analysis of the PNP equations can be further reduced to a 1D analytical approximation for long diodes (aspect ratio, $a/L > 1$), leading to explicit formulas for the currents in the open and closed states as well as the rectification degree for both types of diodes. The important finding of our work is a strong dependence of the diodes' performance on the channel length. Thus, to achieve the best performance, the diodes must have small radii and have to be quite long so that the diode resistance is dominant. Nevertheless, even for diodes that are only a few nanometers long, the rectification exists even when the reservoir walls are neutral and is quite high when the reservoir walls have the same charge as the corresponding sides of the channel. Therefore, the ionic diodes with dimensions as small as 1 nm or less (application of the continuum analysis is questionable for dimensions less than 1 nm) can demonstrate a high rectification performance in a broad range of biases. Nevertheless, this behavior is greatly affected by the edge effects at the entrances and thus such diodes cannot be treated as independent entities in constructing nanofluidic circuits; the reservoirs connecting such elements have to be included and may be the limiting factor in minimizing the dimensions of ionic nonlinear devices.

METHODS

The numerical calculations using the PNP equations were performed (with the help of Comsol Multiphysics 3.3a/3.4 package) for nanochannels connected to cylindrical reservoirs with a length of 1 μm and a 1 μm radius at each opening, whose surfaces were presumed to be neutral for the majority of cases.

Very fine 0.1 nm triangular mesh was used close to the charged walls. Elsewhere, meshing was reduced to the point when no change in ionic current was observed upon further mesh decrease. Ionic current was calculated by integration of the full set of eq 1 solution (PNP-NS) over the chosen nanochannel cross section or by integration over the reservoir borders facing the bulk (Lagrange multipliers integration was used for the latter case). In the case of PNP approximation, the solution velocity was set zero, $u = 0$. The UMFPACK solver was used for solving all described systems; the relative tolerance was set to 10^{-6}.

The dielectric constant was kept constant, $\epsilon = 80$, and the diffusion coefficients, D_i, were presumed identical and equal 2×10^{-9} m^2/s for both ions. The mobilities of the ions were calculated as $\mu_i = eD_i/k_BT$, where k_B is the Boltzmann constant.

The electrical potential on the outmost borders in the left and right reservoirs were set to 0 and V, respectively, as shown in Figure 1. The boundary condition, $d\varphi/dr|_{r=a} = \sigma/\varepsilon\varepsilon_0$, is applied at the walls. At the reservoir walls facing bulk solution, the boundary condition $C = C_{bulk}$ was applied for both ions. For the Navier−Stokes equation, the solution velocity at the walls was set to zero, $u(a) = 0$, and the density and viscosity of pure water, $\rho = 1000$ kg/m^3 and $\nu = 1$ mPa · s, were used.

Acknowledgment. This work was supported in part by the National Science Foundation (CHE 0747237), the RCE Pacific Southwest (Z.S.S.) and by the National Institutes of Health (NIH S06 GM008136) (S.N.S.). The authors are grateful to Eric Kalman for careful reading of the manuscript.

Supporting Information Available: Detailed description of UP diode selectivity, currents in the closed state, and the depletion zone for BP and UP diodes. Concentration dependence of the reverse current for a UP diode and $Q(V)$ for very short diodes are shown as well. Edge effects on BP and UP diodes' performance are presented in detail, considering diodes with charged reservoirs and different charge distributions on the internal pore walls. This material is available free of charge *via* the Internet at http://pubs.acs.org.

REFERENCES AND NOTES

1. Nishizawa, M.; Martin, C. R.; Menon, V. P. Metal Nanotubule Membranes with Electrochemically Switchable Ion-Transport Selectivity. *Science* **1995**, *268*, 700–702.
2. Plecis, A.; Schoch, R. B.; Renaud, P. Ion Transport Phenomena in Nanofluidics: Experimental and Theoretical Study of the Exclusion-Enrichment Effect on a Chip. *Nano Lett.* **2005**, *5*, 1147–1155.
3. Siwy, Z. S. Ion-Current Rectification in Nanopores and Nanotubes with Broken Symmetry. *Adv. Funct. Mater.* **2006**, *16*, 735–746.
4. Karnik, R.; Duan, C.; Castelino, K.; Daiguji, H.; Majumdar, A. Rectification of Ionic Current in a Nanofluidic Diode. *Nano Lett.* **2007**, *7*, 547–551.
5. Vlassiouk, I.; Siwy, Z. Nanofluidic Diode. *Nano Lett.* **2007**, *7*, 552–556.
6. Ramirez, P.; Gomez, V.; Cervera, J.; Schiedt, B.; Mafe, S. Ion Transport and Selectivity in Nanopores with Spatially Inhomogeneous Fixed Charge Distributions. *J. Chem. Phys.* **2007**, *126*, 194703.
7. Coster, H. G. L. A Quantitative Analysis of the Voltage−Current Relationships of Fixed Charge Membranes and the Associated Property of "Punch-Through". *Biophys. J.* **1965**, *5*, 669–686.
8. Bassignana, I. C.; Reiss, H. Ion Transport and Water Dissociation in Bipolar Ion Exchange Membranes. *J. Membr. Sci.* **1983**, *15*, 27–41.
9. Mafe, S.; Ramirez, P. Electrochemical Characterization of Polymer Ion-Exchange Bipolar Membranes. *Acta Polym.* **1997**, *48*, 234–250.
10. Rubinstein, I.; Rubinstein, I. Bipolar Polymeric Arrangements on Electrodes. *J. Phys. Chem.* **1987**, *91*, 235–241.
11. Daiguji, H.; Oka, Y.; Shirono, K. Nanofluidic Diode and Bipolar Transistor. *Nano Lett.* **2005**, *5*, 2274–2280.
12. Daiguji, H.; Yang, P.; Majumdar, A. Ion Transport in Nanofluidic Channels. *Nano Lett.* **2004**, *4*, 137–142.
13. Kalman, E.; Vlassiouk, I.; Siwy, Z. Nanofluidic Bipolar Transistor. *Adv. Mater.* **2008**, *20*, 293–297.
14. Karnik, R.; Fan, R.; Yue, M.; Li, D.; Yong, P.; Majumdar, A. Electrostatic Control of Ions and Molecules in Nanofluidic Transistors. *Nano Lett.* **2005**, *5*, 943–948.
15. Fan, R.; Yue, M.; Karnik, R.; Majumdar, A.; Yang, P. Polarity Switching and Transient Responses in Single Nanotube Nanofluidic Transistors. *Phys. Rev. Lett.* **2005**, *95*, 086607.
16. Karnik, R.; Castelino, K.; Majumdar, A. Field-Effect Control of Protein Transport in a Nanofluidic Transistor Circuit. *Appl. Phys. Lett.* **2006**, *88*, 123114.
17. Li, J.; Stein, D.; McMullan, C.; Branton, D.; Aziz, M. J.;

Golovchenko, J. A. Ion-Beam Sculpting at Nanometre Length Scales. *Nature* **2001**, *412*, 166–169.
18. Storm, A. J.; Chen, J. H.; Ling, X. S.; Zandbergen, H. W.; Dekker, C. Fabrication of Solid-State Nanopores with Single-Nanometre Precision. *Nat. Mater.* **2003**, *2*, 537–540.
19. Dekker, C. Solid-State Nanopores. *Nat. Nanotechnol.* **2007**, *2*, 209–215.
20. Kim, M. J.; Wanunu, M.; Bell, D. C.; Meller, A. Rapid Fabrication of Uniformly Sized Nanopores and Nanopore Arrays for Parallel DNA Analysis. *Adv. Mater.* **2006**, *18*, 3149–3153.
21. Gracheva, M. E.; Vidal, J.; Leburton, J.-P. p−n Semiconductor Membrane for Electrically Tunable Ion Current Rectification and Filtering. *Nano Lett.* **2007**, *7*, 1717–1722.
22. Gracheva, M. E.; Leburton, J.-P. Electrolytic Charge Inversion at the Liquid−Solid Interface in a Nanopore in a Doped Semiconductor Membrane. *Nanotechnology* **2007**, *18*, 145704.
23. Vidal, J.; Gracheva, M. E.; Leburton, J.-P. Electrically Tunable Solid-State Silicon Nanopore Ion Filter. *Nanoscale Res. Lett.* **2007**, *2*, 61–68.
24. Ho, C.; Qiao, R.; Heng, J. B.; Chatterjee, A.; Timp, R. J.; Aluru, N. R.; Timp, G. Electrolytic Transport Through a Synthetic Nanometer-Diameter Pore. *Proc. Natl. Acad. Sci. U.S.A.* **2005**, *102*, 10445–10450.
25. Chen, P.; Mitsui, T.; Farmer, D.; Golovchenko, J.; Gordon, R.; Branton, D. Atomic Layer Deposition to Fine-Tune the Surface Properties and Diameters of Fabricated Nanopores. *Nano Lett.* **2004**, *4*, 1333–1337.
26. Alcaraz, A.; Ramirez, P.; Garcia-Gimenez, E.; Lopez, L.; Andrio, A.; Aguilella, V. M. A pH-Tunable Nanofluidic Diode: Electrochemical Rectification in a Reconstituted Single Ion Channel. *J. Phys. Chem. B* **2006**, *110*, 21205–21209.
27. Miedema, H.; Vrouenraets, M.; Wierenga, J.; Meijberg, W.; Robillard, G.; Eisenberg, R. A Biological Porin Engineered into a Molecular, Nanofluidic Diode. *Nano Lett* **2007**, *7*, 2886–2891.
28. Behrens, S. H.; Borkovec, M. Electrostatic Interaction of Colloidal Surfaces with Variable Charge. *J. Phys Chem. B* **1999**, *103*, 2918–2928.
29. Behrens, S. H.; Borkovec, M. Exact Poisson−Boltzmann Solution for the Interaction of Dissimilar Charge-Regulating Surfaces. *Phys. Rev. E* **1999**, *60*, 7040–7048.
30. Corry, B.; Kuyucak, S.; Chung, S.-H. Tests of Continuum Theories as Models of Ion Channels. II. Poisson−Nernst−Planck Theory *versus* Brownian Dynamics. *Biophys. J.* **2000**, *78*, 2364–2381.
31. Moy, G.; Corry, B.; Kuyucak, S.; Chung, S.-H. Tests of Continuum Theories as Models of Ion Channels. I. Poisson−Nernst−Planck Theory *versus* Brownian Dynamics. *Biophys. J.* **2000**, *78*, 2349–2363.
32. Rice, C. L.; Whitehead, R. Electrokinetic Flow in a Narrow Cylindrical Capillary. *J. Phys. Chem.* **1965**, *69*, 4017–4024.
33. Petsev, D. N.; Lopez, G. P. Electrostatic Potential and Electroosmotic Flow in A Cylindrical Capillary Filled with Symmetric Electrolyte: Analytic Solutions in Thin Double Layer Approximation. *J. Colloid Interface Sci.* **2006**, *294*, 492–498.
34. Vlassiouk, I.; Smirnov, S.; Siwy, Z. S. Ion Selectivity of Single Nanochannels *Nano Lett.* **2008**, *8*, 1978–1985.
35. Sokirko, A. V.; Ramirez, P.; Manzanares, J. A.; Mafe, S. Modeling of Forward and Reverse Bias Conditions in Bipolar Membranes. *Ber. Bunsen-Ges. Phys. Chem* **1993**, *97*, 1040–1049.
36. Ashcroft, N. W.; Mermin, N. D. *Solid State Physics*; Brooks Cole: New York, 1976.
37. Li, S. S. *Semiconductor Physical Electronics*, 2nd ed.; Springer: Berlin, 2006.